Smart Mater. Struct. 7 (1998) 199–208. Printed in the UK PII: S0964-1726(98)90265-8

Structural monitoring by curvature analysis using interferometric fiber optic sensors

D Inaudi†‡, S Vurpillot†, N Casanova†‡ and P Kronenberg†

† IMAC—Laboratory of Stress Analysis, Swiss Federal Institute of Technology, CH-1015 Lausanne, Switzerland§
‡ SMARTEC SA, Via al Molino, CH-6916 Grancia, Switzerland‖

Received 16 October 1996, accepted for publication 4 June 1997

Abstract. All structures undergo deformations under the effects of loads or degradation of the constituent materials. The deformations of any structure (bridges, dams, frames, shells, tunnels, towers, wings, trusses,...) contain a lot of information about its health state. By measuring these deformations it is possible to analyse the loading and aging behavior of the structure. The presented method analyses a structure by subdividing it into sections and cells. The deformation of each of these macro-elements is first analysed separately to obtain local information about the materials, and then combined to provide insight on the global behavior. Examples of these techniques applied to civil engineering structures fitted with long-gage-length fiber optic sensors show the variety of information that can be obtained using this powerful analysis technique.

1. Introduction

The importance of monitoring all structures of some significance is clear [1]. Monitoring is fundamental in order to guarantee the safety of a structure and its users (think of a dam, a bridge or an airplane). It also helps in the planning of maintenance intervention and to increase the knowledge of its real behavior, permitting the optimization of future similar structures.

The monitoring of a new or existing structure can be approached either from the material or from the structural point of view. In the first case, monitoring will concentrate on the local properties of the materials used (e.g., concrete, steel, timber, composite materials, etc) and observe their behavior under load, temperature variations or aging. Short base length strain sensors are the ideal transducers for this type of monitoring approach. If a very large number of these sensors are installed at different points, it is possible to extrapolate information about the behavior of the whole structure from these local measurements.

In the structural approach, the structure is observed from a geometrical point of view. By using long gage length deformation sensors with measurement bases much larger than the characteristic dimensions of the materials (for example a few meters for a concrete bridge), it is possible to gain information about the deformations of the whole structure and extrapolate on the global behavior of the construction materials. The structural monitoring approach will detect material degradation like cracking or flow only if they have an impact on the shape of the structure. This approach usually requires a reduced number of sensors when compared to the material monitoring approach. The availability of reliable strain sensors like resistance strain gages or, more recently, fiber Bragg gratings [2] has historically concentrated most research efforts in the direction of material monitoring rather than structural monitoring. This latter has usually been realized using external measuring methods like triangulation, dial gages and invar wires. Interferometric fiber optic sensors offer an interesting means of implementing structural monitoring with internal or embedded sensors.

The analysis of the measurements obtained by these sensors requires a specific approach compared to the one generally used for strain gages. In the method presented in this article, the structure is first subdivided into sections that undergo simple deformations and then further segmented into cells that contain only a few sensors and where the structural behavior is assumed to be linear. By combining the measurements obtained from the sensors of each cell, section and finally of the whole structure we will obtain information about the local and global behavior of the structure under test.

The deformations can be the result of a variety of direct or indirect agents. Examples include known forces applied to the structure to test it or unknown forces like traffic, wind, earthquakes or snow. Deformations can also be the result of changes in the materials constituting the structures

§ Tel: +41 (21) 693 24 54; fax: +41 (21) 693 47 48; e-mail: inaudi@imac.dgc.epfl.ch; WWW: http://imacwww.epfl.ch
‖ E-mail: inaudi@smartec.ch; WWW: http://www.smartec.ch

0964-1726/98/020199+10$19.50

like cracking, flow, relaxation or a change of temperature. We will see that even if the forces acting on the structure are not known, it is nevertheless possible to extract a great amount of information about the structure's behavior.

2. Structures, sections and cells

In a structure undergoing complex deformations, it is often necessary to install a large number of sensors to obtain useful information. This presents two major difficulties: it is first necessary to decide the number, size and position of the sensors to be installed and then to analyse the huge data flow that results from the measurements. The deformations measured by each single sensor rarely give useful information. Only an appropriate correlation between the values obtained by a much larger number of sensors, and sometimes all of them, generates data that can be correlated to observable quantities like the vertical displacement of a bridge or the crack widths in a concrete beam. The analysis method presented here helps both in the engineering of the sensor network and in the analysis of the resulting measurements.

The main principle of this method consists in subdividing the structure into a number of macro-elements that undergo relatively simple deformations. These sections are further segmented into cells containing only a few sensors or even a single one. To get more insight into this process we will concentrate on beam-like structures that are much larger in one dimension than in the other two. Examples of these structures include bridges, trusses, towers, frames and arches. The principle can, however, be extended to plate-like structures like shells, domes, shell-dams [3], slabs and wings [4].

The first step requires the structure to be subdivided into sections. Each section is supposed to have a constant or continuously varying inertia, a constant load across its length and the introduction of local forces and supports only at its ends (see figure 1). If the behavior of the materials in a section can be considered as homogeneous (e.g., no local cracking), the polynomial degree that best approximates its deformation is determined either analytically or using finite-element programs. If a degree $N + 2$ is found to approximate satisfactorily the deformation of the section, it will be subdivided into N cells. For a beam with constant inertia the deformation is a polynomial of fifth degree and three cells are therefore necessary [5]. For sections with variable inertia, it is sometimes useful to use cells with variable size.

If local variations of the material behavior are expected, more cells are needed. In this case the number N and the size of the cells will be determined in such a way that the material properties inside each single cell can be considered to be reasonably constant. The deformation of the section will in this case be approximated by a polynomial of at most $N + 2$ degrees.

2.1. Cell analysis

The sensors inside a single cell will be used to determine the local behavior of the materials and the global behavior of the cell itself. The sensors will generally be positioned parallel to the beam axis at different heights (see figure 1). The base length of the sensors can be shorter than the cell length, but the best precision is usually obtained with sensors having the same length as the cells. The most relevant parameters that can be analysed at the cell level are the following:

2.1.1. Mean curvature. The radius of curvature of the cell gives an indication of its bending. To obtain this value it is necessary to install one or more sensors at different distances from the neutral axis.

Considering the Bernoulli law on an element dx of the beam, for the simple flexion, the equation of curvature is expressed as:

$$\frac{1}{r(x)} = -\frac{\epsilon(x)}{y} \tag{1}$$

where r is the curvature radius, x the curvilinear abscissa, ϵ the strain in the x direction and y the distance from the neutral axis.

A displacement gage, installed parallel to the neutral axis, measures the deformation over a gage length L. The integration of (1) gives:

$$\frac{1}{L_0}\int_0^L \frac{dx}{r(x)} = -\frac{1}{L}\left(\int_0^L \epsilon(x)dx\right)\Big/ y \Rightarrow \frac{1}{r_m} = \frac{-\Delta L}{yL} \tag{2}$$

where r_m is the mean curvature radius and ΔL is the deformation measured by the sensor after loading.

Equation (2) shows that a displacement gage, placed parallel to the neutral axis, measures the mean curvature $1/r_m$ of the cell. In the case of composed flexion and temperature variations, it is easy to show that a pair of displacement gages, placed at different distances parallel to the neutral axis, are necessary to measure the mean curvature of a cell. In this case the curvature will be given by:

$$\frac{1}{r_m} = \frac{\Delta L_2 - \Delta L_1}{(y_1 - y_2)L} \tag{3}$$

where ΔL_1 and ΔL_2 are the deformations measured by the two sensors, L their gage length and $y_{1,2}$ their vertical position inside the cell, all relative to a common arbitrary origin (for example the bottom of the beam).

2.1.2. Neutral axis position. The position of the neutral axis in a cell can be an indication of the local cracking state [6] of the beam or of its pre-stressing. It can be calculated by:

$$e = \frac{y_1\Delta L_2 - y_2\Delta L_1}{\Delta L_2 - \Delta L_1} \tag{4}$$

where e is the neutral axis position.

2.1.3. Strain diagram. If more than two sensors are placed at different vertical positions inside the cell it is possible to draw a strain diagram. This type of diagram shows the measured mean strain (obtained by dividing the measured deformation by the sensor length) as a function of the height in the beam. It is especially useful for

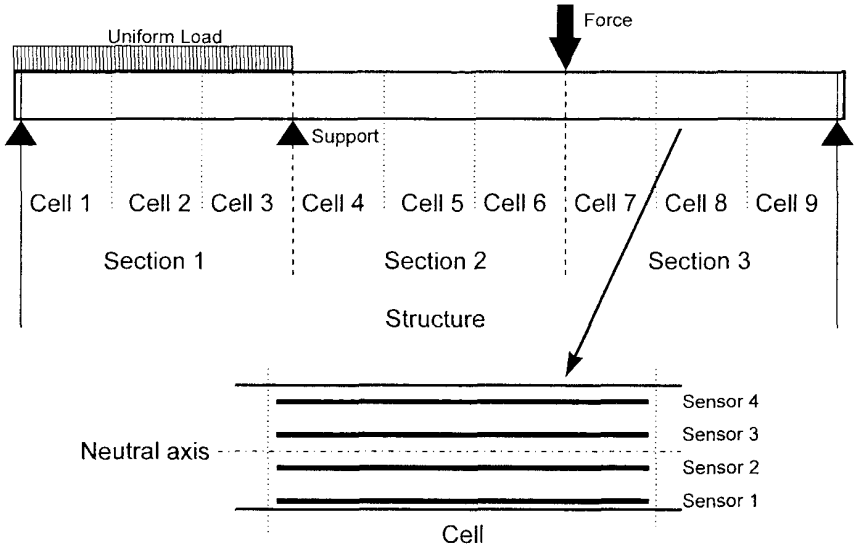

Figure 1. Subdivision of a structure into sections and cells and placement of the sensors inside the cell.

composite or mixed structures where the cohesion between different materials has to be evaluated (see for example section 4.1). This type of diagram also gives the ratio between the elastic moduli of the materials. If the different materials are supposed to work in traction or compression, the strain diagram will show if these suppositions are verified in reality. The position of the neutral axis can also by determined looking at this type of diagram.

2.2. Section analysis

After analysing each cell separately we obtain an estimation of the curvature and the position of the neutral axis as a function of the curvilinear abscissa along the beam length. From the local curvatures it is possible to obtain the section's curvature function by fitting the cell's curvature values to a polynomial of the appropriate degree. For a simple beam section the curvature function is a second degree polynomial of the form:

$$P_2(x) = ax^2 + bx + c \tag{5}$$

where the lower index refers to the degree of the polynomial.

Since the polynomial $P_2(x)$ has three unknowns, only three independent measurements (i.e. cells) are necessary to retrieve it for a single beam section.

The values a, b ,c are then expressed by a trivial linear equation system:

$$\left[\int_{x_A^i}^{x_B^i} (ax^2 + bx + c)\,\mathrm{d}x\right]\left(x_B^i - x_A^i\right)^{-1} = \left.\frac{1}{r_i}\right|_{i=1.2.3} \tag{6}$$

where $1/r_i$ is the mean curvature on $[x_A^i; x_B^i]$ (the beginning and the end of the ith cell). By solving this system for a, b, c we obtain the continuous curvature of the section. If the number of cells exceeds the polynomial degree chosen for the curvature function, the system should be solved by the least-squares method.

The curvature function can give interesting information on the section behavior. For example, in the case of local cracking, the curvatures will concentrate at the position of the cracks. The curvature function also indicates if a momentum is present at the section ends and gives the relative strength between the forces acting on the structure.

2.3. Structure analysis

By combining the curvature function of each section i we can now calculate the curvature of the whole structure and obtain its deformation by double integration.

Equation (5) is the curvature function of adjacent sections. We retrieve the displacement functions by integrating them. Furthermore, the continuity of the displacement function and its first derivative has to be guaranteed at the borders. The displacement functions are expressed by:

$$P_4^i(x) = \int\int P_2^i(x)\,\mathrm{d}x^2 + \alpha^i x + \beta^i \tag{7}$$

where α^i and β^i are the constants of the double integration that satisfy the system:

$$P_4^i\left(x_B^i\right) = P_4^{i+1}\left(x_A^{i+1}\right) \qquad \Big|_{i\in[1;n-1]} \tag{8}$$

$$\frac{\mathrm{d}P_4^i}{\mathrm{d}x}\left(x_B^i\right) = \frac{\mathrm{d}P_4^{i+1}}{\mathrm{d}x}\left(x_A^{i+1}\right) \qquad \Big|_{i\in[1;n-1]} \tag{9}$$

$$P_4^1\left(x_A^1\right) = 0 \qquad P_4^n\left(x_B^n\right) = 0 \tag{10}$$

where n is the number of sections. Equation (8) guarantees the continuity of the deformation, equation (9) the continuity of the slopes, while equation (10) ensures the absence of displacement at the extremities of the structures. This system has two unknowns for each of the n sections. The system has $((n-1)+(n-1)+2) = 2n$ equations. Therefore, the solution is unique.

We have determined that only three displacement sensors, set at different places in each beam section, are

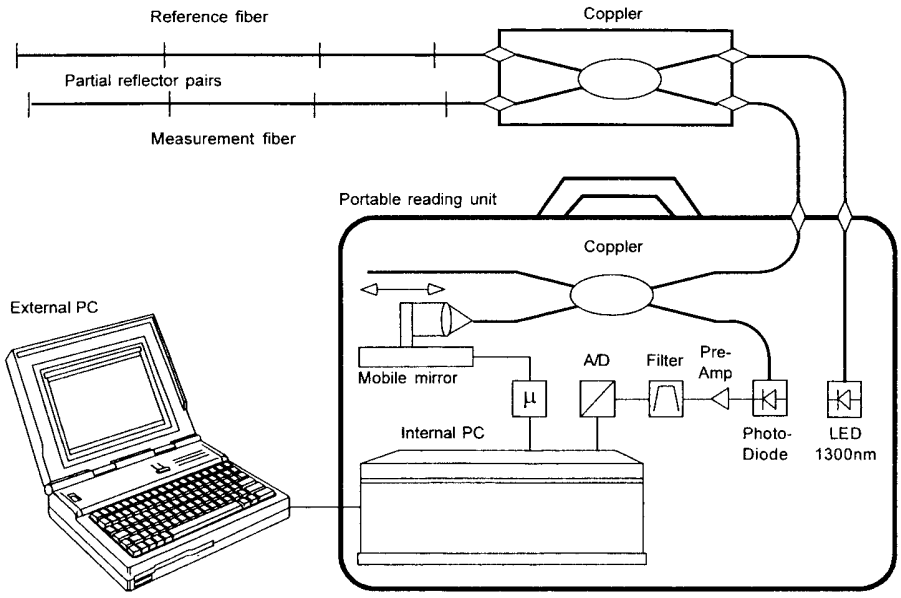

Figure 2. Set-up of the SOFO system.

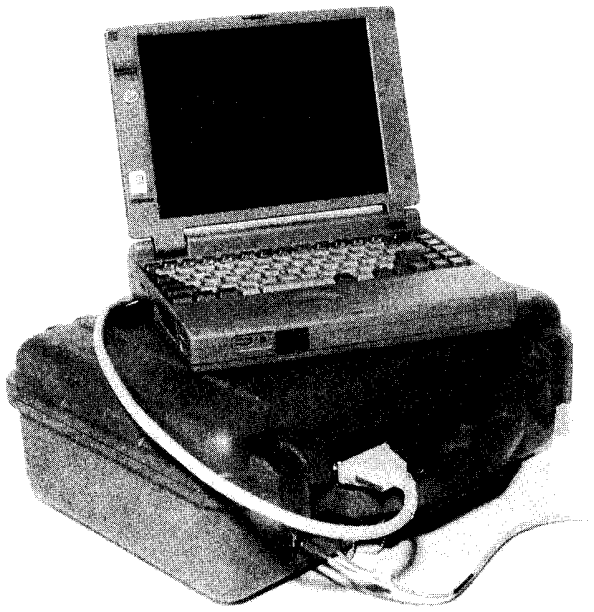

Figure 3. SOFO reading unit with its control portable PC.

sufficient to determine the exact displacement of the whole beam. The whole beam is subdivided into sections of constant inertia and elastic response, uniformly loaded and with additional loads (force, moment, support, etc) only at the extremities.

The general hypotheses are the satisfaction of the Bernoulli conservation law (stating that plane sections remain plane after loading) and the knowledge of the border condition at the extremities of the whole structure. The first hypothesis is satisfied in most cases, while the second is generally irrelevant. Engineers are interested in the structure's internal stresses. These stresses are only generated by relative internal displacements of the structure. This means that the model is able to calculate the deformation of the beam but not its rigid-body displacements in space. This justifies the arbitrary choice of equation (10). To obtain information about the rigid-body displacements, internal sensors are obviously useless and other measurements relative to fixed external points or absolute sensors (like GPS, inclinometer, hydrostatic leveling system, etc) should be carried out. The minimum number of sensors to be placed in the structure depends on the number of parameters needed to retrieve its curvature. One sensor is sufficient for the simple flexion, a pair of sensors are necessary for the composed flexion and one additional sensor per section of beam is sufficient for a triangular load. An increased number of sensors usually increases the measurement precision while adding a certain redundancy useful in the case of sensor failures.

3. Deformation sensors

The deformation sensors used to carry out the analysis described in the previous paragraphs can be based on a large number of techniques: inductive sensors, dial gages, vibrating chords, and so on. However, fiber optic sensors are the ideal choice for many applications, being easy to handle, dielectric, immune to EM disturbances and able to accommodate deformations up to a few percent. The precision requirements, the long gage lengths and the stability required by this application, point to the use of interferometric schemes. However, due to their incremental nature, most interferometric set-ups require continuous and uninterrupted monitoring, which is a major drawback for long-term applications. Low-coherence interferometry offers most of the advantages of interferometric sensors but features non-incremental operation allowing absolute measurements to be performed at any given time. Our laboratory has developed the SOFO monitoring system,

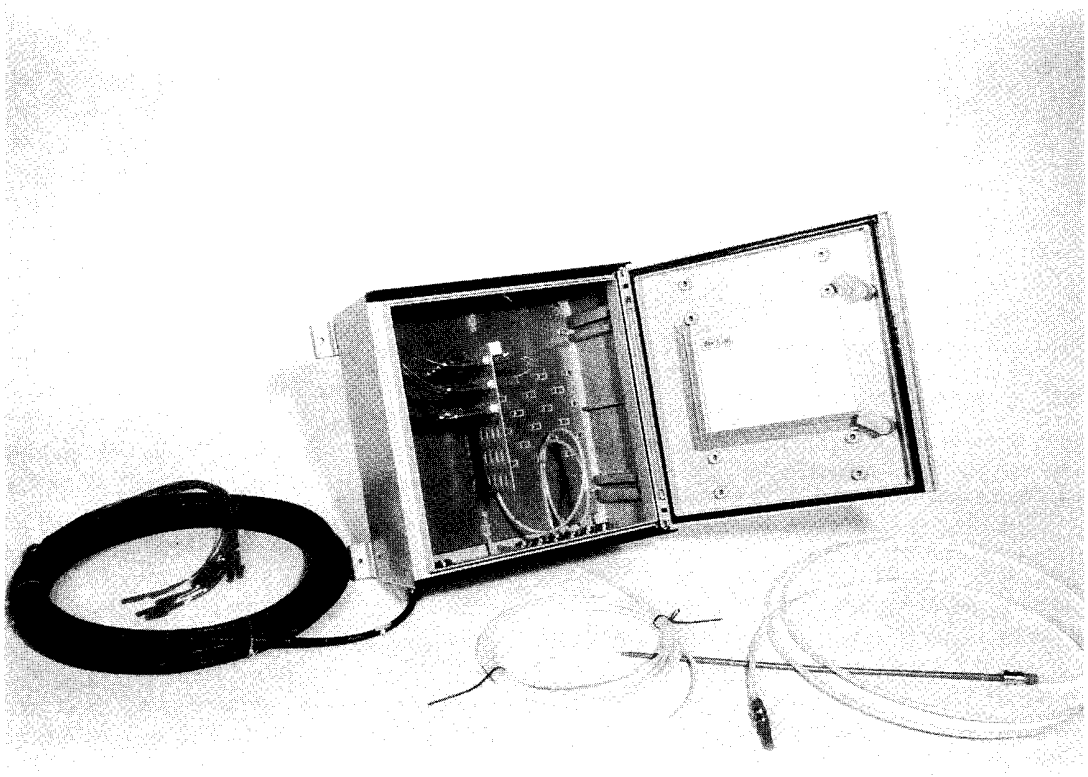

Figure 4. Sensor for concrete embedding. The same sensors can also be surface mounted on existing structures.

based on low-coherence interferometry and particularly adapted to the long-term monitoring of civil structures.

SOFO is the French acronym of Surveillance d'Ouvrages par Fibres Optiques (or structural monitoring by optical fibers). The proposed measurement set-up is based on a double, all-fiber, Michelson interferometer in tandem configuration (see figure 2) [7]. The 1.3 μm radiation of a light emitting diode (LED) with a rated power of 0.2 mW and a coherence length of 30 μm is launched into a single-mode fiber and split, by means of a monomode coupler, into a pair of fibers called the reference and the measurement fiber, respectively. The measurement fiber is mechanically coupled to the structure and follows its deformations, while the reference fiber is installed freely inside a pipe and acts as a temperature reference. The light is reflected by mirrors at the end of the fibers or by a series of partial reflector pairs installed at different fiber locations, which allows the sensors to be multiplexed in-line [8]. The analyser is a Michelson interferometer with one of the arms terminated with a mobile mirror. It allows the introduction of an accurately known path difference between its two arms. The signal detected by the photodiode is pre-amplified and demodulated by a band-pass filter and a digital envelope filter. For each pair of partial reflectors a triple coherence peak is observed. The central peak is obtained when the Michelson analyser is balanced, whereas the side peaks correspond to the mirror positions where the path imbalance between the analyser arms corresponds to the length difference between two twin partial reflectors or the end mirrors. The central peaks from all partial reflectors will thus overlap to a peak of higher intensity, while the lateral peaks will in general appear at different locations. By following the position of each side peak it is possible to determine the total deformation undergone by the measurement fiber between the corresponding partial reflectors and the coupler. The position of the peaks can be determined with a precision of about 2 μm by computing the center of gravity of the peaks themselves.

The main characteristics of the SOFO system are:

(i) Gage length: 20 cm to 8 m for each sensor section. Up to 50 m with special sensors. Up to six sections per chain.

(ii) Resolution: 2 μm, independent of the gage length.

(iii) Dynamic range (maximum measurable deformation): 1% in elongation and shortening (sensors). Up to 150 mm in elongation and shortening (reading unit).

(iv) Precision: better than 0.2% of the measured deformation.

(v) Measurement speed: less than 10 s for each sensor chain.

(vi) Stability: drift not observable over at least three years.

(vii) Other characteristics: rugged, portable and battery-powered reading unit. Sensors adapted to direct concrete embedding or surface mounting on existing structures.

The measurements can either be performed manually, by connecting the different sensors one after the other, or automatically by means of an optical switch. Since the measurement of the length difference between the fibers is absolute, there is no need to maintain a permanent connection between the reading unit and the sensors. A single unit can therefore be used to monitor multiple sensors

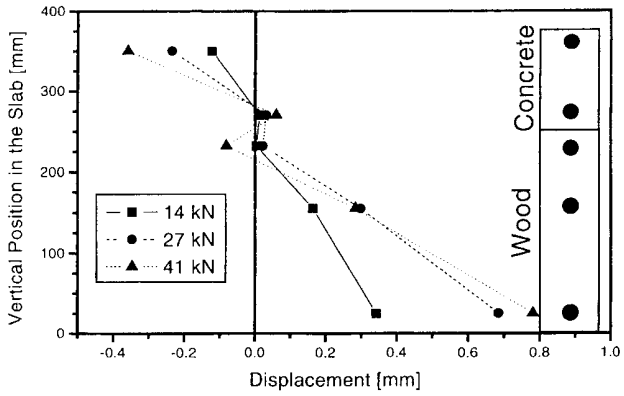

Figure 5. Strain diagram of a mixed timber–concrete slab. At high loading, the typical z-shaped diagram indicates a degradation of the cohesion between the two materials.

and structures with the desired frequency. Figure 3 shows the portable reading unit with the control PC.

Figure 4 shows a typical sensor for lengths up to 8 m. This sensor is adapted to direct concrete embedding or surface mounting on existing structures [9]. The passive region of the sensor is used to connect the sensor to the reading unit and can be up to a few kilometers long.

4. Application examples

The following paragraphs present some of the application examples of the SOFO system where a structural analysis was performed at the level of a cell, a section or the whole structure.

4.1. Cell analysis: timber–concrete slab

A timber–concrete slab offers many interesting advantages when compared to a simple concrete slab. The lower side of the slab is made of wood and withstands mainly tensile stresses, while the upper side is made of concrete and is mainly subject to compressive stresses. Both materials therefore work at their best, the lower timber part also acting as a framework during construction. To guarantee the optimal functioning of this composite structure it is necessary to ensure that the shear forces are transmitted from one material to the other. Otherwise, wood and concrete will lose adherence and work as separate slabs, losing the advantages cited above.

In this experiment, a 13 m long and 1 m wide slab was built. The cohesion was ensured by a series of grooves in the timber beams composing the slab and by a series of metallic bolts. Several fiber optic sensors were placed at different heights in both materials and measured the deformations of the four central meters of the composite slab under four point bending. Figure 5 shows the strain diagram obtained at different loadings. At low loads, the diagram is almost linear, indicating an excellent bond between timber and concrete. The position of the neutral axis near the interface between the materials confirms the soundness of the design. At higher loads, the diagram becomes z-shaped indicating that the cohesion between the two materials is degrading. Because of the complexity of this structure, a large number of sensors were installed in a single cell in order to retrieve precious data about the local behavior of the composite slab. If a similar array of sensors had been placed near the ends of the slab where the shear forces are greater, different diagrams would have been obtained.

4.2. Cell analysis: Moesa railway bridge

The Moesa (Switzerland) railway bridge is a composite steel concrete bridge on three spans of 30 m each. The 50 cm thick concrete deck is supported on the lower flanges of two continuous, 2.6 m high I-beams. The bridge has been constructed alongside an old metallic bridge. After demolishing this one, the new bridge has been moved a distance of 5 m by four hydraulic jacks and positioned on the four refurbished piles of the old bridge.

During the bridge push, which extended over six hours, the more than 20 embedded and surface mounted sensors monitored the curvature variations in the horizontal plane due to the uneven progression of the jacks. Excessive curvature and the resulting cracking of concrete could be ruled out as a result of these measurements. Figure 6 shows the results obtained by two 2 m long sensors placed parallel to the bridge length, at the position of the second pile and placed on the left and on the right of the bridge. Interestingly, most deformations are symmetrical on the two sensors indicating a simple bending of the bridge.

Figure 7 shows the elongation of the bridge (obtained by averaging the left and right sensors) and its curvature (obtained by subtracting the two values and dividing by the sensor gage length and separation). The elongation is mainly due to the heating action of the sun on the bridge. The bending is largely due to the uneven progression of the four jacks. The eight successive pushing phases are clearly recognizable (as well as the lunch break) by the corresponding negative peaks in the curvature plot. After each push phase the bridge was re-aligned by operating the jacks separately. The slight increase of curvature during the day is probably due to the direct sunshine on one of the sides of the bridge. This example shows that even with only two sensors it is possible to retrieve a lot of information about the bridge behavior during a delicate construction phase.

4.3. Section analysis: Lutrive highway bridge

The Lutrive (Switzerland) north and south bridges are two parallel twin bridges. Each one supports two lanes of the Swiss national highway RN9 between Lausanne and Vevey. Built in 1972 by the corbelling method with central articulations, the two bridges are gently curved (r = 1000 m) and each bridge is approximately 395 m long on four spans. The two bridges have the same cross-section. It consists of a box girder of variable height (from 2.5 m to 8.5 m) and two slightly asymmetric cantilevers, meant to reduce the effect of torsion in the curved bridges.

The fourth span of the south bridge, fitted, since 1988, by the IBAP-EPFL Laboratory with a hydrostatic leveling

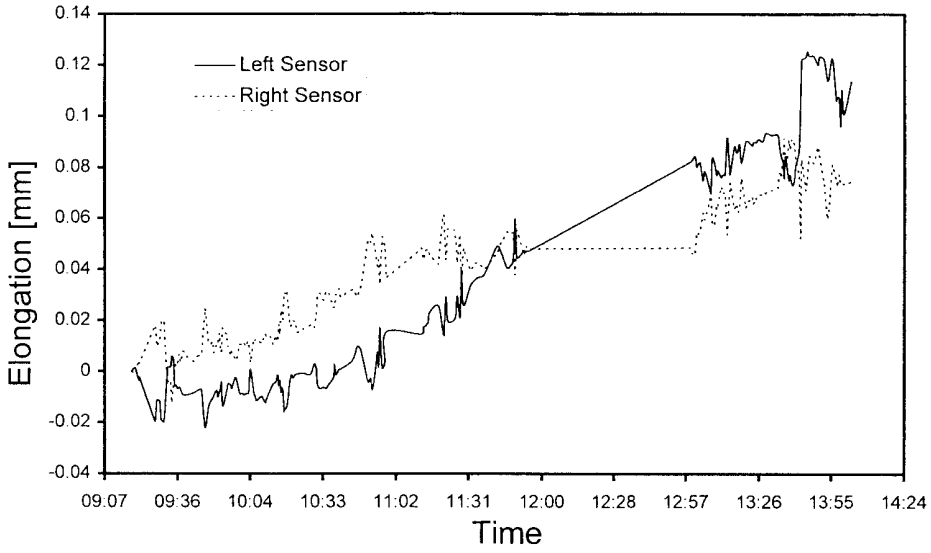

Figure 6. Moesa bridge: deformation measurement from two sensors placed symmetrically on the left and right side of the bridge.

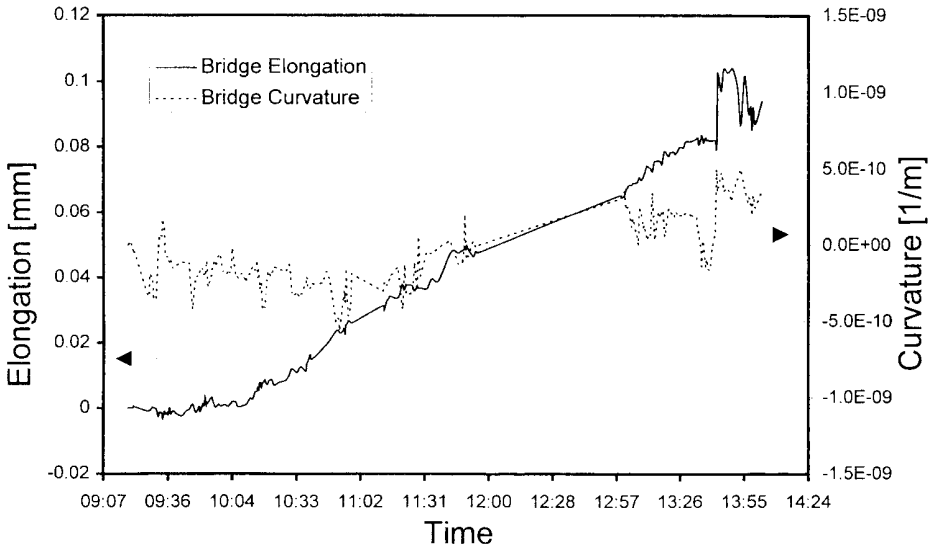

Figure 7. Moesa bridge: curvature and elongation during the bridge push.

system measuring vertical displacements, was chosen to test the algorithm. The static system of this span is considered to be like a cantilever beam with a variable height. To measure the curvatures, six displacement sensors were placed in the interior of the box girder, forming three cells. Curvatures were measured with sensors placed near the top and the bottom of the bridge web and the vertical displacements are retrieved by double integration of the curvature.

Measurements were taken during the 24 h between the 6th of July 1996 at 14h00 to the 7th of July 1996 at 14h00. The temperature difference measured between the upper and the lower slab oscillated between 2.4 °C and 5 °C. Measurements were performed for each 20 min each 2 h, without stopping the traffic, sometimes necessitating a few trials before the bridge regained its calm after the passing of heavy vehicles.

The curvature evolution during 24 h, shown in figure 8, presents a cycle correlated to the temperature difference variations in the bridge. The temperature of the bridge was slightly higher after 24 h. This non-periodicity is retrieved on the curvature measurements. Taking into account the measurements obtained by an inclinometer placed 10 m from the articulation and a null displacement on the pile as the boundary conditions for the double integration, the shape deformation $V(x)$ is calculated for each temporal measurement. This function $V(x, t)$ presents the vertical displacement of a point of co-ordinate x for each discrete measure at a time t. Figure 9 shows the temporal comparison between the vertical displacements calculated with the fiber optic sensors and the hydrostatic leveling system for a point placed at quarter span. The hydrostatic leveling precision can be estimated to be about ± 0.5 mm. The precision on the vertical displacement

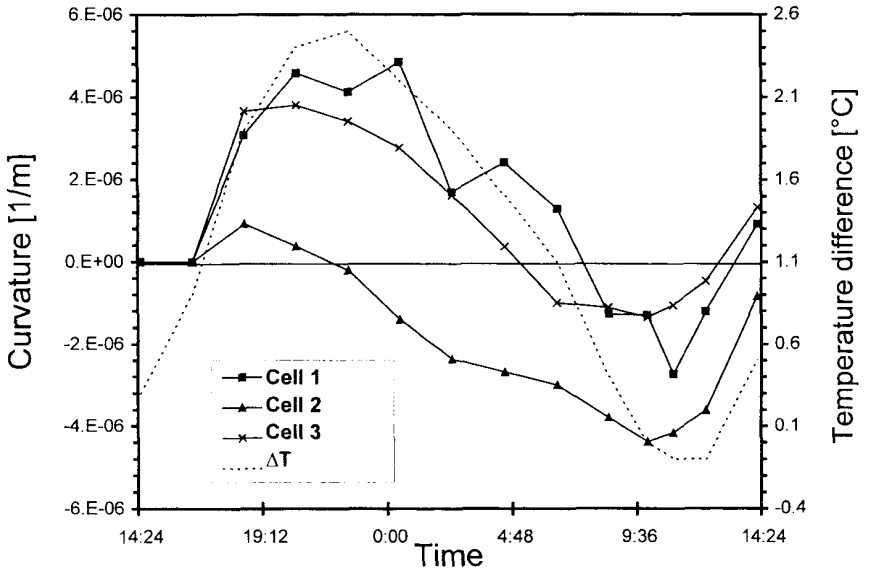

Figure 8. Lutrive bridge: curvature and temperature difference evolution during 24 h.

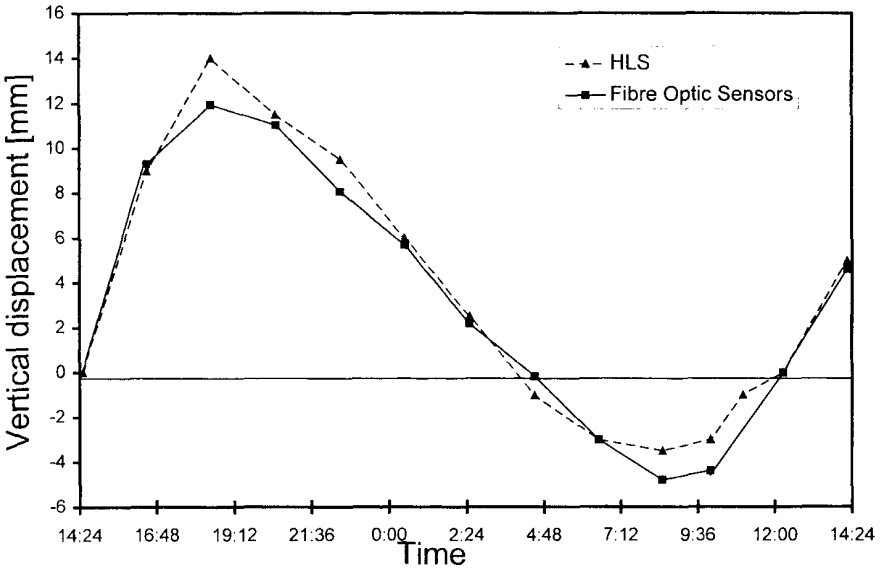

Figure 9. Lutrive bridge: comparison between the vertical displacement retrieved by the fiber optic sensors and the one measured with the hydrostatic leveling system (HLS).

determined by the mathematical model can be obtained by a sensibility study of the model. Considering a precision of 10 μm for the reading unit, 2 cm for the vertical placement of the sensor, 2 cm for the sensors length and 10^{-5} rad for the inclinometer precision, a standard deviation of 20 μm is obtained. This example shows the possibility of obtaining precise information about the vertical displacement of a single bridge span using only a reduced number of displacement sensors. A precision much higher than the one obtained by external measuring systems like optical or hydrostatic leveling can be achieved.

4.4. Structure analysis: timber beam

A load test has been carried out on a 6 m long timber beam with a 112 × 156 mm^2 section on three supports. It was instrumented with 12 fiber optic deformation sensors of the SOFO system organized into four chains of three sensors each. The beam is installed on two or three supports and was divided in two sections. To retrieve the exact deformation, the curvature had to be measured in each section of beam in three different places. Each section was therefore divided into three cells. In each cell, two optical fiber sensors measured the elongation or the shortening above and below the neutral axis (assuming a constant temperature, only one sensor per cell would have been necessary). Throughout the different load conditions, the beam deformation calculated by the algorithm was compared to the real deformation monitored by four dial gages installed under the beam. When present, the central support, not explicitly considered by the algorithm, acted

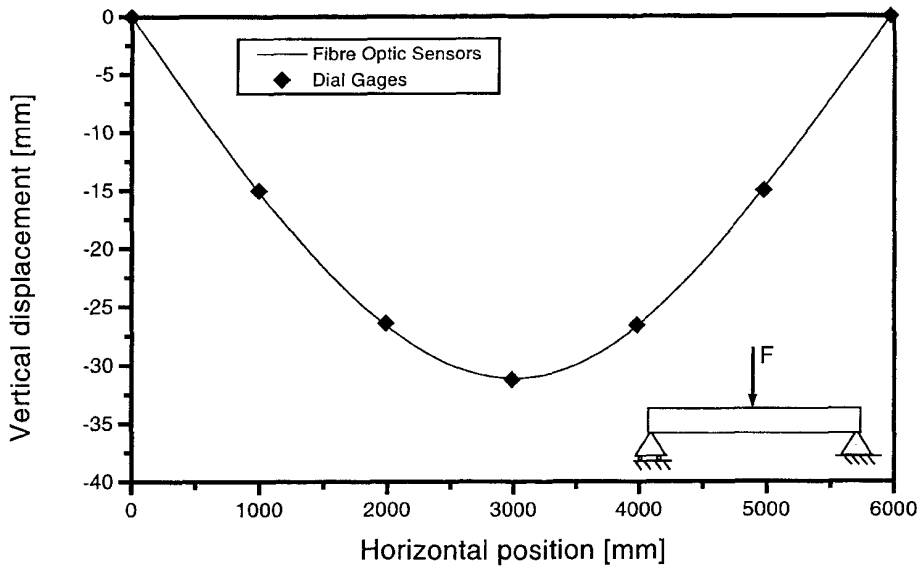

Figure 10. Timber beam on two supports with central loading. Comparison between the vertical displacements retrieved by the fiber optic sensors and the one measured by dial gages.

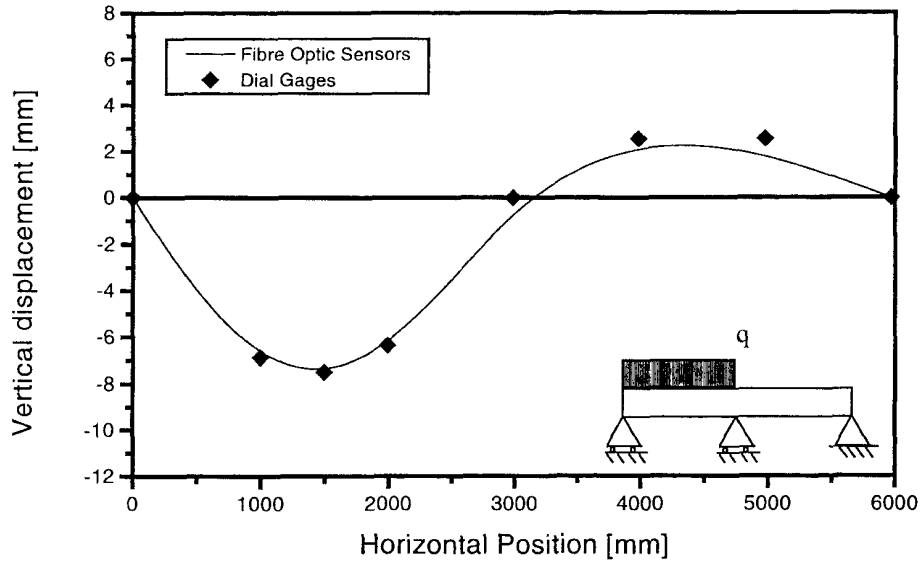

Figure 11. Timber beam on three supports with uniform load on one span. Comparison between the vertical displacements retrieved by the fiber optic sensors and the one measured by dial gages.

as a fifth point of comparison. Two typical results are presented: beam on two supports punctually loaded (figure 10) and beam on three supports uniformly loaded on one span (figure 11). These two figures show a comparison between the calculated displacements and the ones measured directly with the dial gages. The results show an excellent correspondence in the first case (global error less than 1%) as well as in the second case (global error less than 8%). In this case, the existence of the central support was retrieved by the model. The difference of precision between the two cases was expected, since the first loading case needs at least four curvature measurements, while the second case needs six in order to retrieve the exact vertical displacement. Six measurements were available in both cases, so that the information exceeds the minimal requirements for the first load case, allowing better precision. The measured displacements in the two cases were between the ratios [(l/200); (l/400)] while the prescriptions impose a maximum displacement of l/300 for many civil structures (l being the span length).

A similar experiment was performed on a 6 m long concrete beam submitted to four-point bending. In this case, the vertical displacement could be retrieved with a precision of better than 1%, even when the beam was heavily cracked. This shows that the presented analysis method works well even outside the elastic domain.

4.5. Structure analysis: Versoix highway bridge

The Versoix (Switzerland) twin bridges are situated between the cities of Geneva and Lausanne on a heavily trafficked

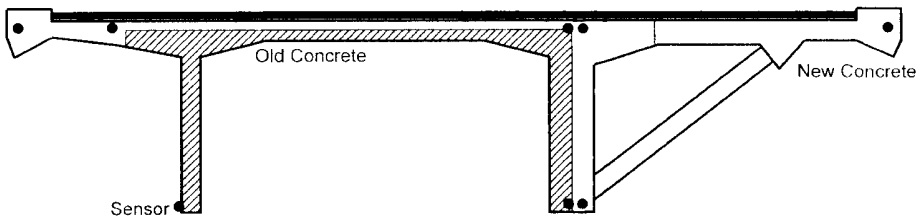

Figure 12. Sensor placement inside the cross-section of one cell in the Versoix bridge. Thirteen cells cover two bridge spans and allow the retrieval of the horizontal and vertical displacements.

section of the Swiss highway network. To increase its security it was decided to enlarge this concrete bridge from the 1960s by adding a cantilevered slab on the external side of both bridges. Because of the added weight and pre-stressing, as well as the differential shrinkage between old and new concrete, it is expected that the bridge will bend during the construction phases both horizontally and vertically. To monitor these deformations it was decided to install more than one hundred SOFO sensors subdivided into 13 cells covering two of the six spans of one bridge. Each cell contains height sensors as shown in figure 12. This disposition should also permit the evaluation of the bridge torsion and the evaluation of the adherence between the new and the old concrete.

Once the bridge refurbishing is terminated, the sensor network will remain in place to perform long-term monitoring, diagnostics and remote monitoring via telephone or Internet networks.

5. Conclusions

The proposed method helps in the design and in the analysis of the measurements obtained by a network of deformation sensors. By dividing the structure into macro-elements it is possible to retrieve information about both its local and global behavior. Fiber optic sensors based on low-coherence interferometry proved ideal to implement this concept in the case of civil structures. The presented application examples show the power of the technique, the great amount of information and the precision that can be obtained even with a reduced number of sensors. More complex applications require tens or even hundreds of sensors. In this case, automatic data analysis tools will prove indispensable to treat the huge data flow that will result from the measurements. The analysis of the curvature function of a beam-like structure can provide information that is not directly accessible with strain or displacement measurements.

Finally, the permanent monitoring will increase the security of the structure and allow a better planning of the maintenance interventions at a reasonable cost.

Acknowledgments

The authors are indebted to L Pflug, M Pedretti, R Passera, P Colombo, S Marazzi, R Delez, G Krüger, A Scano, R Emery, R Spataro, O Burdet, M Lehmann and the whole IMAC, IMM and DIAMOND teams for their precious help, support and interesting discussions.

This research program is conducted under the financial support of the Swiss CTI (Commission pour la Technologie et l'Innovation) and the Board of the Swiss Federal Institutes of Technology.

References

[1] Wen Y K 1991 Intelligent structures 2; monitoring and control *Int. Workshop on Intelligent Systems (Perugia, Italy, 27–29 June 1991)*

[2] Maaskant R, Alavie T, Measures R M, Ohn M, Karr S, Glennie D, Wade C, Tadros G and Rizkalla S 1994 Fiber optic Bragg grating sensor network installed in a concrete road bridge *Proc. SPIE Smart Structures and Materials 1994: Smart Sensing, Processing, and Instrumentation* **2191** 457–65

[3] Kronenberg P, Casanova N, Inaudi D and Vurpillot S 1997 Dam monitoring with fiber optic sensors *Smart Structures and Materials (San Diego, February, 1997)*

[4] Poh S and Baz A 1996 Distributed sensor for rectangular plates *Proc. SPIE Smart Structures and Materials (San Diego, February, 1996)* **2718** 355

[5] Vurpillot S, Inaudi D and Scano A 1996 Mathematical model for the determination of the vertical displacement from internal horizontal measurements of a bridge *Proc. SPIE Smart Structures and Materials (San Diego, February, 1996)* **2719-05**

[6] Abdunur C 1994 Monitoring of bridges subject to transversal cracks *Proc. SPIE 2nd Eur. Conf. on Smart Structures and Materials (Glasgow, October, 1994)* vol 2361, pp 156–9

[7] Inaudi D, Elamari A, Pflug L, Gisin N, Breguet J and Vurpillot S 1994 Low-coherence deformation sensors for the monitoring of civil-engineering structures *Sensors Actuators* A **44** 125–30

[8] Inaudi D 1995 Coherence multiplexing of in-line displacement and temperature sensors *Opt. Eng.* **34**

[9] Inaudi D, Vurpillot S, Casanova N and Osa-Wyer A 1996 Development and field test of deformation sensors for concrete embedding *Proc. SPIE Smart Structures and Materials (San Diego, February, 1996)* **2721-16**